Proceedings of the ASME 2007 International Design Engineering Technical Conferences & Computers and Information in Engineering Conference
IDETC/CIE 2007
September 4-7, 2007, Las Vegas, Nevada, USA

DETC2007/VIB-35197

PARETO OPTIMAL STRUCTURAL MODELS AND PREDICTIONS CONSISTENT WITH DATA AND MODAL RESIDUALS

Evaggelos Ntotsios
Department of Mechanical & Industrial Engineering

Konstantinos Christodoulou
Department of Mechanical & Industrial Engineering

Costas Papadimitriou*
Department of Mechanical & Industrial Engineering

Systems Dynamics Laboratory,
University of Thessaly, Volos 38334, Greece

ABSTRACT

A multi-objective identification method for model updating based on modal residuals is proposed. The method results in multiple Pareto optimal structural models that are consistent with the measured modal data, the class of models used to represent the structure and the modal residuals used to judge the closeness between the measured and model predicted modal data. The conventional single-objective weighted modal residuals method for model updating is also used to obtain Pareto optimal structural models by varying the values of the weights. Theoretical and computational issues related to the solution of the multi-objective and single optimization problems are addressed. The model updating methods are compared and their effectiveness is demonstrated using experimental results obtained from a three-story laboratory structure tested at a reference and a mass modified configuration. The variability of the Pareto optimal models and their associated response prediction variability are explored using two structural model classes, a simple 3-DOF model class and a higher fidelity 546-DOF finite element model class. It is shown that the Pareto optimal structural models and the corresponding response predictions may vary considerably. The variability of Pareto optimal structural model is affected by the size of modelling and measurement errors. This variability reduces as the fidelity of the selected model classes increases.

1 INTRODUCTION

Structural model updating methods (e.g. Mottershead and Friswell 1993; Farhat and Hemez 1993) have been proposed in the past to reconcile mathematical models, usually discretized finite element models, with modal data obtained from experimental modal analysis. The optimal structural models resulting from such methods can be used for improving the model response and reliability predictions (Papadimitriou et al. 2001) and structural health monitoring applications (Sohn and Law 1997; Fritzen et al. 1998). The estimate of the optimal model is sensitive to uncertainties that are due to limitations of the mathematical models used to represent the behavior of the real structure, the presence of measurement and processing error in the modal data, the number and type of measured modal data used in the reconciling process, as well as the norms used to measure the fit between measured and model predicted modal properties.

Structural model parameter estimation problems based on measured modal data (e.g. Bohle and Fritzen 2003) are often formulated as weighted least-squares problems in which modal metrics, measuring the residuals between measured and model predicted modal properties, are build up into a single weighted modal residuals metric formed as a weighted average of the multiple individual modal metrics using weighting factors. Standard optimization techniques are then used to find the optimal values of the structural parameters that minimize the single weighted residuals metric representing an overall measure of fit between measured and model predicted modal properties. Due to model error and measurement noise, the results of the optimization are affected by the values assumed for the weighting factors.

The model updating problem has also been formulated in a multi-objective context (Haralampidis et al. 2005) that allows the simultaneous minimization of the multiple modal metrics, eliminating the need for using arbitrary weighting factors for weighting the relative importance of each modal metric in the overall measure of fit. In contrast to the conventional weighted least-squares fit between measured and model predicted modal data, the multi-objective parameter estimation methodology provides multiple Pareto optimal structural models consistent with the data in the sense that the fit each Pareto optimal

* Professor and author of correspondence, Phone: (30) 24210-74006, Fax: (30) 24210-74012, Email: costasp@uth.gr.

model provides in a group of measured modal properties cannot be improved without deteriorating the fit in at least one other modal group. These multiple Pareto optimal structural models are due to modelling and measurement errors.

In this work, the structural model updating problem using modal residuals is first formulated as a multi-objective optimization problem and then as a single-objective optimization with the objective formed as a weighted average of the multiple objectives using weighting factors. Theoretical issues arising in multi-objective identification are addressed and the correspondence between the multi-objective identification and the weighted modal residuals identification is established. Computational issues associated with solving the resulting multi-objective and single-objective optimization problems are also addressed, including issues related to the estimation of global optima. Theoretical and computational issues are illustrated by applying the methodology for updating two model classes, a simple 3-DOF model and a much higher fidelity finite element model class, using experimentally obtained modal data from a small-scaled three-story laboratory steel building structure tested at a reference and a mass modified configuration using modal data. Validation studies are performed to show the applicability of the methodologies and the advantages of the multi-objective identification. Emphasis is given in investigating the variability of the Pareto optimal models and the variability of the response predictions from these Pareto optimal models. Results demonstrate the effect of model error on model updating and model prediction variability.

2 MODEL UPDATING BASED ON MODAL RESIDUALS

Let the measured modal data from a structure consist of modal frequencies $\hat{\omega}_r$ and modeshape components $\hat{\underline{\phi}}_r \in R^{N_0}$ at N_0 measured DOFs, $r = 1, \cdots, m$, where m is the number of observed modes. Consider a parameterized class of linear structural models used to model the dynamic behavior of the structure and let $\underline{\theta} \in R^{N_\theta}$ be the set of free structural model parameters to be identified using the measured modal data. Let also $\omega_r(\underline{\theta})$ and $\underline{\phi}_r(\underline{\theta}) \in R^{N_d}$, where N_d is the number of model degrees of freedom (DOF), be the predictions of the modal frequencies and modeshapes obtained for a particular value of the parameter set $\underline{\theta}$ by solving the eigenvalue problem corresponding to the model mass and stiffness matrices $M(\underline{\theta})$ and $K(\underline{\theta})$, respectively.

The objective in a modal-based structural identification methodology is to estimate the values of the parameter set $\underline{\theta}$ so that the modal data predicted by the linear class of models best matches, in some sense, the experimentally obtained modal data. For this, the measured modal properties are first grouped into n groups g_i, $i = 1, \cdots, n$. Each group contains one or more modal properties. For the i th group g_i, a norm $J_i(\underline{\theta})$ is introduced to measure the residuals of the difference between the measured values of the modal properties involved in the group and the corresponding modal values predicted from the model class for a particular value of the parameter set $\underline{\theta}$. This difference is due to modeling and measurement errors, always present in structural identification problems.

The grouping of the modal properties into n groups and the selection of the measures of fit (residuals) $J_1(\underline{\theta}), \cdots, J_n(\underline{\theta})$ are usually based on user preference. Specifically, let

$$J_{\omega_r}(\underline{\theta}) = \frac{[\omega_r(\underline{\theta}) - \hat{\omega}_r]^2}{[\hat{\omega}_r]^2} \tag{1}$$

$$J_{\underline{\phi}}(\underline{\theta}) = \frac{\left\| \beta_r L_0 \underline{\phi}_r(\underline{\theta}) - \hat{\underline{\phi}}_r \right\|^2}{\left\| \hat{\underline{\phi}}_r \right\|^2} \tag{2}$$

$r = 1, \cdots, m$, be the measures of fit (residuals) between the N_D measured set of modal data and the model predicted modal data for the r-th modal frequency and modeshape components, respectively, where $\| \underline{z} \|^2 = \underline{z}^{\mathrm{T}} \underline{z}$ is the usual Euclidian norm and $\beta_r = \hat{\underline{\phi}}_r^T L_0 \underline{\phi}_r / \left\| L_0 \underline{\phi}_r \right\|^2$ is a normalization constant that guaranties that the measured modeshape $\hat{\underline{\phi}}_r$ at the measured DOFs is closest to the model modeshape $\beta_r L_0 \underline{\phi}_r(\underline{\theta})$ predicted by the particular value of $\underline{\theta}$. The matrix $L_0 \in R^{N_0 \times N_d}$ is an observation matrix comprised of zeros and ones that maps the N_d model DOFs to the N_0 observed DOFs.

Among the various grouping schemes available, the following are considered for illustration purposes. A grouping scheme may be defined so that each group contains one modal property, the modal frequency or the modeshape for each mode. In this case, there are $n = 2m$ measures of fit given by $J_i(\underline{\theta}) = J_{\omega_i}(\underline{\theta})$ and $J_{m+i}(\underline{\theta}) = J_{\underline{\phi}}(\underline{\theta})$, $i = 1, \cdots, m$. More general grouping schemes can be defined by forming n groups g_i, $i = 1, \cdots, n$, with each group containing a number of modal properties. The measure of fit in a modal group is the sum of the individual measures of fit in (1) for the corresponding modal properties involved in the modal group. The modal properties assigned to each group are selected by the user according to their type and the purpose of the analysis.

A grouping scheme is next defined by grouping the modal properties into two groups as follows. The first group contains all modal frequencies with the measure of fit $J_1(\underline{\theta})$ selected to represent the difference between the measured and the model predicted frequencies for all modes, while the second group contains the modeshape components for all modes with the measure of fit $J_2(\underline{\theta})$ selected to represents the difference between the measured and the model predicted modeshape

components for all modes. Specifically, the two measures of fit are given by

$$J_1(\underline{\theta}) = \frac{1}{m}\sum_{r=1}^{m} J_{\omega_r}(\underline{\theta}) \quad \text{and} \quad J_2(\underline{\theta}) = \frac{1}{m}\sum_{r=1}^{m} J_{\underline{\phi}}(\underline{\theta}) \tag{3}$$

The aforementioned grouping scheme is used in the application section for demonstrating the features of the proposed model updating methodologies.

2.1 Multi-Objective Identification:

The problem of identifying the model parameter values that give the best fit in all groups of modal properties is formulated as a multi-objective optimization problem stated as follows (Haralampidis et al. 2005). Find the values of the structural parameter set $\underline{\theta}$ that simultaneously minimizes the objectives

$$\underline{y} = \underline{J}(\underline{\theta}) = (J_1(\underline{\theta}), \cdots, J_n(\underline{\theta})) \tag{4}$$

subject to inequality constrains $\underline{g}(\underline{\theta}) \le \underline{0}$ and parameter constrains $\underline{\theta}_{low} \le \underline{\theta} \le \underline{\theta}_{upper}$, where $\underline{\theta} = (\theta_1, \cdots, \theta_{N_\theta}) \in \Theta$ is the parameter vector, Θ is the parameter space, $\underline{y} = (y_1, \cdots, y_n) \in Y$ is the objective vector, Y is the objective space, $\underline{g}(\underline{\theta})$ is the vector function of constrains, and $\underline{\theta}_{low}$ and $\underline{\theta}_{upper}$ are respectively the lower and upper bounds of the parameter vector $\underline{\theta}$. For conflicting objectives $J_1(\underline{\theta}), \cdots, J_n(\underline{\theta})$, there is no single optimal solution, but rather a set of alternative solutions, known as Pareto optimal solutions, that are optimal in the sense that no other solutions in the parameter space are superior to them when all objectives are considered.

Using multi-objective terminology, the Pareto optimal solutions are the non-dominating vectors in the parameter space Θ, defined mathematically as follows. A vector $\underline{\theta} \in \Theta$ is said to be non-dominated regarding the set Θ if and only if there is no vector in Θ which dominates $\underline{\theta}$. A vector $\underline{\theta}$ is said to dominate a vector $\underline{\theta}'$ if and only if

$$\begin{aligned} &J_i(\underline{\theta}) \le J_i(\underline{\theta}') \quad \forall i \in \{1, \cdots, n\} \quad \text{and} \\ &\exists\ j \in \{1, \cdots, n\}\ :\ J_j(\underline{\theta}) < J_j(\underline{\theta}') \end{aligned} \tag{5}$$

The set of objective vectors $\underline{y} = \underline{J}(\underline{\theta})$ corresponding to the set of Pareto optimal solutions $\underline{\theta}$ is called Pareto optimal front. The characteristics of the Pareto solutions are that the modal residuals cannot be improved in any modal group without deteriorating the modal residuals in at least one other modal group. Specifically, using the objective functions in (3), all optimal models that trade-off the overall fit in modal frequencies with the overall fit in the modeshapes are estimated.

The multiple Pareto optimal solutions are due to modelling and measurement errors. The level of modelling and measurement errors affect the size and the distance from the origin of the Pareto front in the objective space, as well as the variability of the Pareto optimal solutions in the parameter space. For given modelling and measurement error, the Pareto optimal structural models may vary considerably in the parameter space. The variability of the Pareto optimal solutions also depends on the overall sensitivity of the objective functions or, equivalently, the sensitivity of the modal properties, to model parameter values $\underline{\theta}$. The lower the sensitivity to modal properties, the higher the variability of the Pareto optimal models. Such variabilities were demonstrated for the case of two-dimensional objective space and one-dimensional parameter space in the work by (Christodoulou and Papadimitriou 2007).

2.2 Weighted Modal Residuals Identification:

The parameter estimation problem is traditionally solved by minimizing the single objective

$$J(\underline{\theta}; \underline{w}) = \sum_{i=1}^{n} w_i J_i(\underline{\theta}) \tag{6}$$

formed from the multiple objectives $J_i(\underline{\theta})$ using the weighting factors $w_i \ge 0$, $i = 1, \cdots, n$, with $\sum_{i=1}^{n} w_i = 1$. The objective function $J(\underline{\theta}; \underline{w})$ represents an overall measure of fit between the measured and the model predicted modal data. The relative importance of the modal residual errors in the selection of the optimal model is reflected in the choice of the weights. The results of the identification depend on the weight values used. The weight values depend on the adequacy of the model class used to represent structural behavior and the accuracy with which the measured modal data are obtained. However, the choice of weight values is arbitrary since the modeling error and the uncertainty in the measured data are usually not known apriori. Conventional weighted least squares methods assume equal weight values, $w_1 = \cdots = w_n = 1/n$.

It can be readily shown that the optimal solution to the problem (6) is one of the Pareto optimal solutions. Thus, solving a series of single objective optimization problems of the type (6) and varying the values of the weights w_i from 0 to 1, excluding the case for which the values of all weights are simultaneously equal to zero, Pareto optimal solutions are alternatively obtained. These solutions for given $\underline{w}$ are denoted by $\hat{\underline{\theta}}(\underline{w})$. It should be noted, however, that there may exist Pareto optimal solutions that do not correspond to solutions of the single-objective weighted least-squares problem. A severe drawback of generating Pareto optimal solutions by solving the series of weighted single-objective optimization problems by uniformly varying the values of the weights is that this procedure often results in cluster of points in parts of the Pareto front that fail to provide an adequate representation of the entire Pareto shape.

3 COMPUTATIONAL ISSUES

The optimization of $J(\underline{\theta}; \underline{w})$ in (6) with respect to $\underline{\theta}$ for given $\underline{w}$ can readily be carried out numerically using any available algorithm for optimizing a nonlinear function of several variables. These single objective optimization

problems may involve multiple local/global optima. Conventional gradient-based local optimization algorithms lack reliability in dealing with the estimation of multiple local/global optima observed in structural identification problems (Teughels and De Roeck 2003; Christodoulou and Papadimitriou 2007), since convergence to the global optimum is not guaranteed. Evolution strategies (Beyer 2001) are more appropriate and effective to use in such cases. Evolution strategies are random search algorithms that explore better the parameter space for detecting the neighborhood of the global optimum, avoiding premature convergence to a local optimum. A disadvantage of evolution strategies is their slow convergence at the neighborhood of an optimum since they do not exploit the gradient information. A hybrid optimization algorithm should be used that exploits the advantages of evolution strategies and gradient-based methods. Specifically, an evolution strategy is used to explore the parameter space and detect the neighborhood of the global optimum. Then the method switches to a gradient-based algorithm starting with the best estimate obtained from the evolution strategy and using gradient information to accelerate convergence to the global optimum.

The set of Pareto optimal solutions can be obtained by minimizing the objective vector (4) using available multi-objective optimization algorithms. Among them, the evolutionary algorithms, such as the strength Pareto evolutionary algorithm (Zitzler and Thiele 1999; Haralampidis et al. 2005), are well-suited to solve the multi-objective optimization problem. These algorithms process a set of promising solutions simultaneously and therefore are capable of capturing several points along the Pareto front. They are based on an arbitrary initialized population of search points in the parameter space, which by means of selection, mutation and recombination evolves towards better and better regions in the search space. In addition, techniques such as clustering are introduced in the algorithms to uniformly distribute the points along the Pareto front, provided that the values of objective along the Pareto front are of the same order of magnitude.

Another very efficient algorithm for solving the multi-objective optimization problem is the Normal-Boundary Intersection (NBI) method (Das and Dennis 1998) which produce an evenly spread of points along the Pareto front, even for problems for which the relative scaling of the objectives are vastly different. The NBI optimization involves the solution of constrained nonlinear optimization problems using available gradient-based constrained optimization methods.

The strength Pareto evolutionary algorithm, although it does not require gradient information, it has the disadvantage of slow convergence for objective vectors close to the Pareto front (Haralampidis et al. 2005) and also it does not generate an evenly spread Pareto front, especially for large differences in objective functions. The NBI on the other hand uses the gradient information, it has fast convergence for low dimensional objective space and generates an evenly spread Pareto front even for vast differences in objective values.

4 APPLICATIONS

Experimental data from a scaled three-story steel building structure are used to demonstrate the applicability and effectiveness of the proposed model updating methods, as well as investigate the prediction variability of the Pareto optimal structural models. A schematic diagram of the side and the front views of the laboratory structure are given in Figure 1. The floors of the building are made of identical steel beams of hollow orthogonal cross section. The two interstory columns that support each floor are made up of identical thin steel plates. The columns and beams are connected through angles with the help of bolts and nuts. The horizontal members are made to be much stiffer compared to the vertical structural elements so that the structural behaviour can be adequately represented by a shear beam building model. The total height of the structure is approximately 2.4m. The y direction of the frame is made to be stiffer to prevent coupling of motion with the x direction, the latter being the principal direction of interest. The structure is considered as the reference structure and it is denoted by C_0. A second structural configuration is considered by adding concentrated masses in both sides of each floor of the reference structure as shown in Figure 1. The added weight due to the concentrated masses is approximately 9.5 Kg per floor, while the total added mass corresponds to approximately 42% of the mass of the reference structure. The modified structural configuration is denoted by C_1.

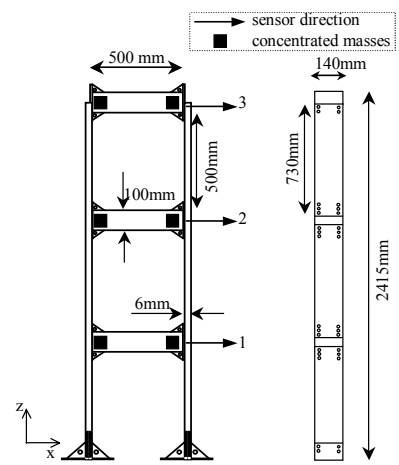

Figure 1. Front and side views of 3-story structure

The modal properties of the two structural configurations C_0 and C_1 are identified from frequency response functions that are obtained by processing the excitation force and acceleration response time histories generated from impulse hammer tests. An array of three acceleration sensors located on the structure as schematically shown in Figure 1, record the acceleration time histories during the test along the x direction. Multiple data sets are generated and processed that correspond to different excitation position of the impulse hammer at the second and third floor of the structure along the

x direction. Table 1 and 2 reports the values of the identified modal frequencies and modeshape components at the measured locations of the lowest three bending modes for the reference $\mathcal{C}_0$ and mass modified $\mathcal{C}_1$ structural configurations.

Table 1. Modal frequencies and modeshapes identified for the reference structural configuration

	Reference Structure $\mathcal{C}_0$		
Mode #	1st	2nd	3rd
Modal Freq. (Hz)	4.646	13.81	19.48
Modeshape Components	1.000	-0.9026	-0.6448
	0.8069	0.3009	1.000
	0.4561	1.000	-0.7801

Table 2. Modal frequencies and modeshapes identified for the mass modified structural configuration

	Reference Structure $\mathcal{C}_1$		
Mode #	1st	2nd	3rd
Modal Freq. (Hz)	3.908	11.57	16.31
Modeshape Components	1.000	-0.8709	-0.5708
	0.8219	0.3528	1.000
	0.4408	1.000	-0.7892

For each structural configuration, the following two parameterised model classes are introduced to represent the behaviour of the structure along the x direction, as well as will be used to investigate the effect of modelling error in model updating and model response prediction variability.

The first model class, which is schematically shown in Figure 2a, is a 3-DOF mass-spring chain model. The modelling is based on the assumptions that the floors of the structure are rigid and that the stiffness is provided by the interstory plates. A lumped mass model is considered. Specifically, the i-th mass of the model includes the mass of the i-th floor and half of the mass of the interstory plates that are attached to the i-th

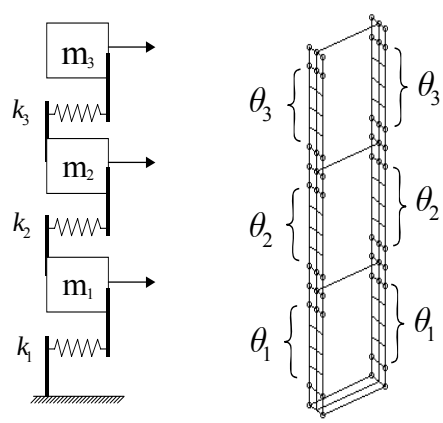

Figure 2. Parameterized (a) 3-DOF and (b) 546-DOF Models

floor. Thus, based on the weights of the structural elements, the masses m_1, m_2 and m_3 are taken to be equal to $m_1 = m_2 = m_0$ and $m_3 = 0.76m_0$, where $m_0 = 22.6$ Kg. The initial (nominal) values of the spring stiffnesses k_{01}, k_{02} and k_{03} are taken to be equal, that is, $k_{01} = k_{02} = k_{03} = k_0$. The ratio k_0 / m_0 between the nominal values of the stiffnesses and masses of the 3-DOF model was selected so as to minimize the difference between the first modal frequency predicted by the model and the first measured modal frequency for the structural configuration $\mathcal{C}_0$.

The 3-DOF mass-spring chain model is parameterized introducing three parameters θ_1, θ_2 and θ_3, one for the stiffness of each spring, modelling the interstory stiffness, so that $k_i = \theta_i k_{0i}$, for $i = 1,2,3$, where $k_{0i} = k_0$ is the nominal value of the stiffness of each spring in the nominal model and k_i is the updated value of the stiffness of each parameterised spring based on the measured data. This parameterized model class is denoted by $\mathcal{M}_0$.

For the modified structure $\mathcal{C}_1$ with added concentrated masses, the same 3-DOF model class is used with modified masses $m_1 + m_1'$, $m_2 + m_2'$ and $m_3 + m_3'$ that take into account the concentrated masses m_1', m_2' and m_3' added on the structure at each floor (see Figure 1). The parameter set $\underline{\theta}$ is kept the same as the one used for the reference structure. This parameterized model class for the modified structural configuration $\mathcal{C}_1$ is denoted by $\mathcal{M}_1$.

The second model class, which is schematically shown in Figure 2b, is a detailed finite element model. Each floor beam is modeled with a beam element, while the columns between each floor are modeled, due to its small thickness, with 12 plate elements each. The sizes of both types of elements are calculated from the structural drawing. The modulus of elasticity and the density are based on the material properties. The plate elements near the joints, between columns and floors, are assumed to be very stiff, in order to model the large rigidity in these parts of the structure. The finite element model developed based on modeling assumptions, the structural drawings and the properties of the materials used, is referred to as the initial (nominal) finite element model. This model consists of 3 beam elements and 72 plate elements (24 elements per story), while the number of DOF is 546.

The 546-DOF finite element model is parameterised introducing three parameters θ_1, θ_2 and θ_3, each one associated with the modulus of elasticity of the thin plate elements of interstory columns, so that $E_i = \theta_i E_{0i}$, for $i = 1,2,3$, where $E_{0i} = E_0$ is the nominal value of the modulus of elasticity of interstory plate elements in the initial finite element model and E_i is the updated value of the modulus of elasticity of each parameterised plate element. This parameterized model class is denoted by $\mathcal{M}_{0,FE}$.

The finite element model of the modified structure with concentrated masses is obtained from the finite element model of the reference structure by adding the known values of the concentrated masses at the edge nodes of the horizontal beam elements used to model the stiffness of the floors. The parameter set $\underline{\theta}$ is kept the same as the one used for the reference structure. This parameterized model class for the modified structural configuration C_1 is denoted by $M_{1,FE}$.

The model within each of the defined model classes with parameter values $\theta_1 = \theta_2 = \theta_3 = 1$ correspond to the initial (nominal) model of the corresponding model classes. It should be emphasized that the three parameters of all four model classes are referred to common interstory stiffness properties of the 3 story structure at the reference and mass modified configurations.

4.1 Structural Model Updating:

Model updating results are computed for the model classes M_0 and $M_{0,FE}$ based on the experimental data in Table 1 available for the reference structural configuration C_0, as well as the model classes M_1 and $M_{1,FE}$ based on the experimental data in Table 2 available for the structural configuration C_1. The Pareto optimal models are estimated from the proposed multiobjective identification method using the NBI algorithm and 20 points along the Pareto front. The optimal models estimated for the edge points defining the CHIM in the NBI multi-objective algorithm are based on the hybrid optimization method combining evolution strategies and gradient based methods. The two objective functions in (3) are used in the model updating results.

The results from the multi-objective identification methodology are shown in Figure 3. For each model class and associated structural configuration, the Pareto front, giving the Pareto solutions in the two-dimensional objective space, is shown in Figure 3a. The non-zero size of the Pareto front and the non-zero distance of the Pareto front from the origin are due to modeling and measurement errors. Specifically, the distance of the Pareto points along the Pareto front from the origin is an indication of the size of the overall measurement and modeling error. The size of the Pareto front depends on the size of the model error and the sensitivity of the modal properties to the parameter values $\underline{\theta}$ (Christodoulou and Papadimitriou 2007). It is observed that the residual errors $J_1(\hat{\underline{\theta}})$ and $J_2(\hat{\underline{\theta}})$ between the measured and the model predicted modal properties obtained from the Pareto optimal models $\hat{\underline{\theta}}$ for the higher fidelity 546-DOF model classes are significantly smaller than the residual errors corresponding to the 3-DOF model classes. Consequently, for the higher fidelity 546-DOF model classes, the Pareto front moves closer to the origin of the objective space. In addition it is observed that the sizes of the Pareto fronts for the 546-DOF model classes reduce to approximately one third of the sizes of the Pareto fronts observed for the 3-DOF model classes. These results certify, at it should be expected based on the modeling assumptions, that the 546 model classes are higher fidelity models than the 3-DOF model classes. Also the results in Figure 3a quantify the quality of fit, acceptance and degree of accuracy of a model class in relation to another model class based on the measure data.

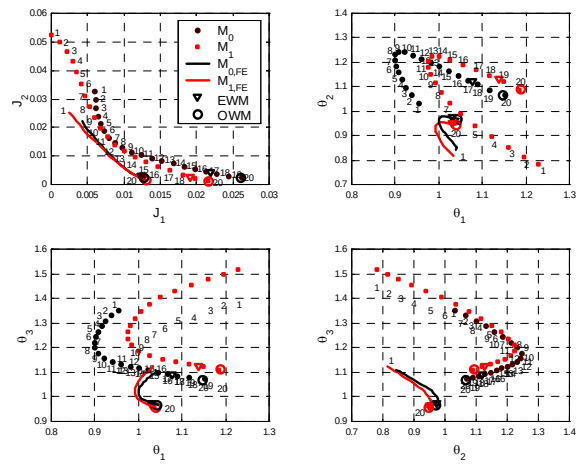

Figure 3. Pareto front and Pareto optimal solutions in the (a) objective space and (b-d) parameter space

Figures 3b-d show the corresponding Pareto optimal solutions in the three-dimensional parameter space. Specifically, these figures show the projection of the Pareto solutions in the two-dimensional parameter spaces (θ_1, θ_2), (θ_1, θ_3) and (θ_2, θ_3). It is observed that a wide variety of Pareto optimal solutions are obtained for both model classes and structural configurations that are consistent with the measured data and the objective functions used. For each model class, the Pareto optimal solutions are concentrated along a one-dimensional manifold in the three-dimensional parameter space. Comparing the Pareto optimal solutions for a model class, it can be said that there is no Pareto solution that improves the fit in both modal groups simultaneously. Thus, all Pareto solutions correspond to acceptable compromise structural models trading-off the fit in the modal frequencies involved in the first modal group with the fit in the modeshape components involved in the second modal groups.

Comparing the Pareto optimal solutions for the 3-DOF model classes M_0 and M_1 corresponding to the two structural configurations C_0 and C_1, respectively, it can be observed that the length of the one-dimensional manifold in the parameter space for the structural configuration C_1 is significantly larger than the length obtained for the structural configuration C_0 which means that the variability of the Pareto optimal solutions for the configuration C_1 is significantly higher than the variability of the Pareto optimal solutions for the configuration C_0. The size of the Pareto front is affected by the sensitivity of the modal properties to the parameter values. The higher the sensitivity, the smaller the size of the Pareto front, which is consistent with the theoretical result presented for the special case of the one-dimensional

parameter space in the work by Christodoulou and Papadimitriou (2007).

Comparing the results for the 546-DOF model classes with the corresponding ones obtained for the 3-DOF model classes, it can be noted that are qualitatively similar. However, the size of the one dimensional optimal solutions manifolds for the 546-DOF model classes $M_{0,FE}$ and $M_{1,FE}$ are significantly smaller than the size of the manifolds for the 3-DOF model classes M_0 and M_1. These results clearly demonstrate that as the fidelity of the model class improves, the variability of the Pareto optimal models reduces. This has important implications in the selection of the weight values used in weighted modal residuals method for model updating and model-based prediction studies. Since the variability of the Pareto optimal solutions reduces as the fidelity of the models improves, the effect of the choice of weight on weighted modal residuals methods diminishes as the fidelity of the model increases.

It should be noted that in the absence of model and measurement errors, the Pareto optimal models from the two common reference model classes referring to the common parameter set should coincide independently of the structural configuration used for obtaining experimental modal data. As the results in Figures 3b-d suggest, the Pareto optimal values of the common parameter set $\underline{\theta}$ of the 3-DOF model classes M_0 and M_1 corresponding to the two structural configurations C_0 and C_1, respectively, differ considerably despite the fact that the parameters for the two common reference model classes refer to the same interstory stiffnesses of the two structural configurations. The differences can be attributed mainly to the size of modeling errors involved in the 3-DOF model classes. Instead, comparing the Pareto optimal values obtained from the 546-DOF model classes $M_{0,FE}$ and $M_{1,FE}$ for the two structural configurations C_0 and C_1, it is observed that the optimal solution manifolds for the 546-DOF model classes are significantly closer than the optimal solution manifolds for the 3-DOF model classes. This certifies that the higher fidelity models provide consistent estimates of the common parameters in common reference model classes introduced to model different structural configurations.

4.2 Predictions Using Pareto Optimal Structural Models:

The purpose of the identification is to construct faithful structural models, within a selected model class, that can be used for making improved structural performance predictions consistent with the measured data. The alternative models obtained along the Pareto front provide different performance predictions that are all acceptable based on the measured data and the measures of fit employed. The variability of these predictions is next explored.

First, the variability in the modal properties predicted by the Pareto optimal models is estimated for the model classes M_0 and $M_{0,FE}$ representing structural configuration C_0, and the model classes M_1 and $M_{1,FE}$ representing structural configuration C_1. The values of the three modal frequencies predicted by the Pareto optimal models are shown in Figure 4.

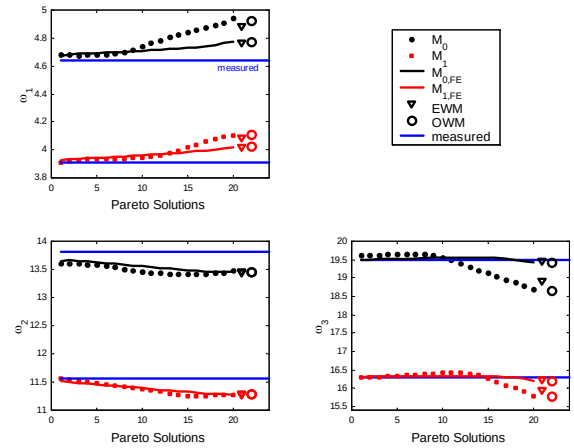

Figure 4. Variability of modal frequencies predicted by the Pareto optimal solutions

The measured modal frequencies for structural configurations C_0 and C_1 are also shown for comparison purposes. The corresponding MAC values between the modeshape components predicted by the Pareto optimal models for each model class and the measured modeshapes for the three bending modes are shown in Figure 5. For each model class, different Pareto optimal models along the Pareto front result in different predictions of the structural modal frequencies and MAC values.

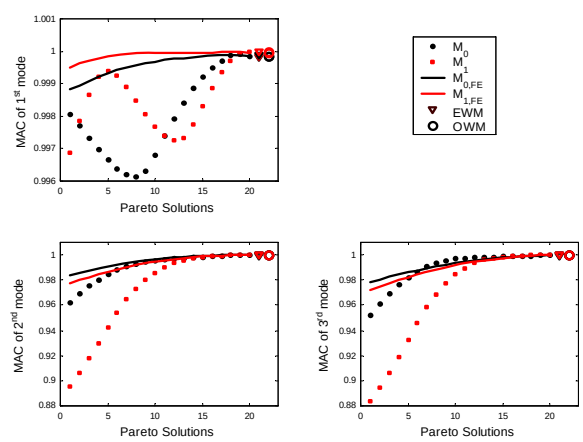

Figure 5. Variability of MAC values predicted by the Pareto optimal solutions

A relatively large variability in the predictions is observed for the 3-DOF model classes M_0 and M_1. The percentage error between the Pareto optimal model predictions for the modal frequencies is as high as 5% for the first modal frequency for both model classes M_0 and M_1. The MAC values vary from

0.88 to values very close to 1.0 for both model classes M_0 and M_1. It is clear that there is a trade off between the fit that the Pareto optimal models for model classes M_0 and $M_{0,FE}$ provide to the modal frequencies and the modeshapes. Specifically, the Pareto models 1 to 10 provide a very good fit to the modal frequencies in the expense of deteriorating the fit in the MAC values to values significantly smaller than one. The Pareto models 11 to 20 for model classes M_0 and $M_{0,FE}$ improve the MAC values to values very close to one in the expense of deteriorating the fit in the modal frequencies.

Comparing the 3-DOF model classes and the 546-DOF model classes, the 546-DOF model classes provide significantly better fit in the modal frequencies than the fit provided by the 3-DOF model classes. Also, comparing the results in Figure 5, it is observed that the higher fidelity 546-DOF model classes give MAC values between the Pareto optimal models and the measurements that are much closer to one than the MAC values obtained for the 3-DOF model class. These results verify that higher fidelity model classes tend to give better predictions that are less sensitive to selections required in model updating, such as the weight values used in weighted residuals methods.

It should be noted that the variability in the Pareto optimal structural models affect considerably the variability in the predictions of other response quantities such as the frequency response function and the probability of failure. The Pareto optimal models can be combined with structural response and reliability prediction tools to quantify such variabilities.

5 CONCLUSIONS

A multi-objective model updating algorithm is proposed to characterize and compute all Pareto optimal models from a model class, consistent with the measured data and the norms used to measure the fit between the measured and model predicted modal properties. Theoretical and computational issues were demonstrated by updating a simple and a higher fidelity model classes using experimental data from two configurations of a scaled three-story steel structure. A wide variety of Pareto optimal structural models consistent with the measured modal data were obtained. The measures of fit values along the Pareto front may vary significantly, at least one order of magnitude. The variability in the Pareto optimal models is due to the model and measurement error. The large variability in the Pareto optimal models resulted in large variability in the structural response predictions. It has been demonstrated that higher fidelity model classes tend to move the Pareto front towards the origin and reduce the size of the Pareto front in the objective space, reduce the size of the Pareto optimal solutions manifold in the parameter space, provide better fit to the measured quantities, and give much better predictions corresponding to reduced variability.

6 ACKNOWLEDGEMENTS

This research was co-funded 75% from the European Union (European Social Fund), 25% from the Greek Ministry of Development (General Secretariat of Research and Technology) and from the private sector, in the context of measure 8.3 of the Operational Program Competitiveness (3rd Community Support Framework Program) under grant 03-EΔ-524 (PENED 2003).

7 REFERENCES

[1] Beyer, H. G., 2001, *The theory of evolution strategies*, Berlin, Springer-Verlag.

[2] Bohle, K., Fritzen, C. P., 2003, "Results obtained by minimizing natural frequencies and MAC-value errors of a plate model", *Mechanical Systems and Signal Processing*, Vol. **17**, pp. 55-64.

[3] Christodoulou, K. and Papadimitriou, C., 2007, "Structural Identification Based on Optimally Weighted Modal Residuals." *Mechanical Systems and Signal Processing*, Vol. **21**, pp. 4-23.

[4] Das, I., J. E. Dennis, Jr., 1998, "Normal-Boundary Intersection: A new method for generating the Pareto surface in nonlinear multi-criteria optimization problems", *SIAM J. Optimization*, Vol. **8**, pp. 631-657.

[5] Fritzen, C. P., Jennewein, D., Kiefer, T., 1998, "Damage detection based on model updating methods", *Mechanical Systems and Signal Processing*, Vol. **12** (1), pp. 163-186.

[6] Farhat, C., Hemez, P. M., 1993, "Updating finite element dynamics models using an element-by-element sensitivity methodology", *AIAA Journal* Vol. **131**, pp. 1702-1711.

[7] Haralampidis, Y., Papadimitriou C., Pavlidou, M., 2005, "Multi-objective framework for structural model identification", *Earthquake Engineering and Structural Dynamics*, Vol. **34** (6), pp. 665-685.

[8] Mottershead, J. E., Friswell, M. I., 1993, "Model updating in structural dynamics: A survey", *Journal of Sound and Vibration*, Vol. **167**, pp. 347-375.

[9] Papadimitriou, C., Beck, J. L., Katafygiotis, L. S., 2001, "Updating robust reliability using structural test data", *Probabilistic Engineering Mechanics*, Vol. **16**, pp. 103-113.

[10] Sohn, H., Law K. H., 1997, "Bayesian probabilistic approach for structural damage detection", *Earthquake Engineering and Structural Dynamics*, Vol. **26**, pp. 1259-1281.

[11] Teughels, A., De Roeck, G., 2003, "Damage detection and parameter identification by finite element model updating", *Archives of Computational Methods in Engineering*, Vol. **12** (2), pp. 123-164.

[12] Zitzler, E., Thiele, L., 1999, "Multi-objective evolutionary algorithms: A comparative case study and the strength Pareto approach", *IEEE Transactions on Evolutionary Computation*, Vol. **3**, pp. 257-271.